Radiat Environ Biophys (2013) 52:531–537
DOI 10.1007/s00411-013-0485-6

SHORT COMMUNICATION

# Microbeam irradiation of *C. elegans* nematode in microfluidic channels

**M. Buonanno · G. Garty · M. Grad · M. Gendrel · O. Hobert · D. J. Brenner**

Received: 30 January 2013 / Accepted: 18 July 2013 / Published online: 13 August 2013


**Abstract** To perform high-throughput studies on the biological effects of ionizing radiation in vivo, we have implemented a microfluidic tool for microbeam irradiation of *Caenorhabditis elegans*. The device allows the immobilization of worms with minimal stress for a rapid and controlled microbeam irradiation of multiple samples in parallel. Adapted from an established design, our microfluidic clamp consists of 16 tapered channels with 10-μm-thin bottoms to ensure charged particle traversal. Worms are introduced into the microfluidic device through liquid flow between an inlet and an outlet, and the size of each microchannel guarantees that young adult worms are immobilized within minutes without the use of anesthesia. After site-specific irradiation with the microbeam, the worms can be released by reversing the flow direction in the clamp and collected for analysis of biological endpoints such as repair of radiation-induced DNA damage. For such studies, minimal sample manipulation and reduced use of drugs such as anesthetics that might interfere with normal physiological processes are preferable. By using our microfluidic device that allows simultaneous immobilization and imaging for irradiation of several whole living samples on a single clamp, here we show that 4.5-MeV proton microbeam irradiation induced DNA damage in wild-type *C. elegans*, as assessed by the formation of Rad51 foci that are essential for homologous repair of radiation-induced DNA damage.

**Keywords** Microbeam irradiation with microfluidic devices · *C. elegans* microbeam irradiation · Small animal microbeam irradiation · Rad51 foci in *C. elegans*

M. Buonanno (✉) · G. Garty · M. Grad · D. J. Brenner
Radiological Research Accelerator Facility, Columbia University, 136 S. Broadway, P.O. Box 21, Irvington, NY 10533, USA
e-mail: mb3591@columbia.edu

M. Gendrel · O. Hobert
Department of Biochemistry and Molecular Biophysics, Howard Hughes Medical Institute, Columbia University Medical Center, New York, NY, USA

## Introduction

*Caenorhabditis elegans* nematode is a well-established research tool suitable for radiobiological studies in vivo. With a transparent body that can be easily observed under a microscope and a relative small diameter (50 μm), *C. elegans* is a particularly advantageous model for microbeam studies (Durante and Friedl 2011). Thanks to the ability to target specific regions of a sample, microbeam irradiation of complex organisms allows to characterize the mechanisms underlying tissue-specific response to radiation, including DNA repair.

DNA double-strand breaks (DSBs) are considered the main cytotoxic lesions directly induced by ionizing radiation [reviewed in (Little 2000)]; faulty processing of DSBs contributes to the induction of both chromosomal abnormalities and gene mutations (Goodhead 1994; Ward 1995). Central to DSBs repair is Rad51 homolog (*S. cerevisiae*) protein that mediates strand invasion and strand exchange between DNA molecules during homologous recombination repair (Sung 1994); at the site of DSBs, Rad51 forms subnuclear complexes that are microscopically detectible as foci, which contain many of the enzymatic activities required for efficient repair of DSBs (Shinohara and Ogawa 1995).

The role of Rad51 in *C. elegans* is well established (Rinaldo et al. 2002, Martin et al. 2005); *rad51* gene

suppression through RNA interference leads to embryonic lethality, decreased fertility (Takanami et al. 1998), and, notably, hypersensitivity to γ-irradiation in both germ and somatic cells (Takanami et al. 2000, Rinaldo et al. 2002).

Models such as *C. elegans* allow elucidating the mechanisms underlying radiation-induced effects in a whole organism in which intact cell-to-cell communication, neuroendocrine signaling, and every aspect of the animal's metabolism are preserved (O'Rourke et al. 2009). Nevertheless, some biological endpoints such as behavioral and functional genomic studies are carried out manually and can be extremely labor-intensive; radiobiological studies with the microbeam (Greubel et al. 2008; Mosconi et al. 2011) furthermore require that living worms remain completely immobile for the duration of the irradiation. This can be achieved by gluing worms with polymers such as cyanoacrylate (Kerr et al. 2000) or by cooling the samples at 4 °C to halt motion (Chung et al. 2008). Alternatively, the worms can be treated with anesthetics; however, these chemicals either do not completely prevent movement, such as in the case of levamisole (Lewis et al. 1980) or can interfere with normal physiological processes, as in the case of sodium azide (Rothman and Singson 2012). In addition to sample immobilization, site-specific irradiation with the microbeam also requires prompt visualization of the target, though this generally involves the use of genetically engineered strains that exhibit fluorescent-tagged molecules that serve as irradiation targets (Bertucci et al. 2009).

In order to facilitate animal manipulation and increase overall throughput of irradiation and imaging capabilities without the use of drugs such anesthetics or other methods that might perturb the normal biochemical state of the organism, researchers have begun to use microfluidics devices for handling *C. elegans* (Hulme et al. 2007; Rohde et al. 2007; Zeng et al. 2008; Gilleland et al. 2010). These tools, which use engineered systems to manipulate and process small volumes of fluids, are commonly made of transparent biocompatible materials making them suitable for observation and handling of living samples such as *C. elegans* that have the ability to grow in liquid. Channel-microfluidics, in particular, allows gentle and reversible mechanical worm immobilization (Shi et al. 2011).

Microfluidic systems can significantly reduce the amount of time-consuming manual operations normally required for *C. elegans* experiments (Hulme et al. 2007). In the context of microbeam irradiation, microfluidic devices ensure that several living samples can be immobilized and irradiated in parallel in an identical and rapid manner.

Inspired by an established design (Hulme et al. 2007), we have implemented a microfluidic tool for microbeam irradiation of 16 *C. elegans* at a time without the use of fluorescent-tagged targets. Supported by this high-throughput irradiation technology, here we show that 4.5 MeV proton microbeam irradiation induces DNA damage in wild-type worms, as assessed by Rad51 foci formation.

## Materials and methods

### Strains and maintenance

Strains were cultured and manipulated as previously described (Brenner 1974). Briefly, worms were continuously fed for many generations and maintained at 20 °C in a temperature-controlled incubator on nematode growth medium (NGM) agar on Petri dishes supplemented with *Escherichia coli* (OP50) as a food source. Both wild-type reference strain N2 Bristol and the *rad51* mutant strain TG9 [*dpy-13(e184) rad51 (Ig8701) IV/nT1[let-?(m435)] (IV;V)*] (Alpi et al. 2003; Martin et al. 2005) were obtained from the *Caenorhabditis* Genetics Center. Plates of unstarved worms were cultured to obtain a homogeneous population of mainly young adults at the time of irradiation. Worm handling occurred in sterile M9 buffer (3 g $KH_2PO_4$, 6 g $Na_2HPO_4$, 5 g NaCl, 1 ml 1 M $MgSO_4$ in 1L $H_2O$).

### Microfluidic worm clamp for microbeam irradiation

Inspired by an established design (Hulme et al. 2007), the worm clamps were fabricated by soft lithography (Xia and Whitesides 1998) at the Columbia University Clean Room. Briefly, the design, consisting of distribution channels to an array of 16 tapered microfluidic channels, was transferred to a photocurable resist (SU-8, Microchem, Newton, MA) using a mask aligner (MA6, Karl Suss, Princeton, NJ) and a chrome mask. Poly(dimethyl siloxane) (PDMS) (Sylgard 184, Dow Corning, Midland, MI) was poured onto the master and cured at 80 °C for 2 h, with a capillary tube embedded for an outlet needle connection. After curing, the chip was cut to size, and holes were punched into the PDMS to create the inlet reservoir and outlet connection. A thin PDMS sealing layer was prepared separately by spinning and curing PDMS onto a silanized silicon wafer at 1,500 rpm for 30 s, yielding a 10-μm-thick layer. The two PDMS layers were irreversibly bonded together after exposure to oxygen plasma (Diener Electronic Tetra-30-LF-PC, Royal Oak, MI) for 30 s. The worm clamps were then irreversibly bonded to a glass slide with a hole drilled for the inlet reservoir that fits into a custom-made holder on the computer-controlled microbeam stage. To prevent the collapse of the thin PDMS layer during operation, glass cover slips were cut to 1 $cm^2$ and bonded to the bottom of the inlet and outlet chambers. Intravenous tubing

terminated with a 23G needle was used to connect the outlet of the channel to a syringe pump (Fusion 200, Chemyx Inc., Stafford, TX) that operated at a rate of 50 µl/min with a 3-cc syringe. The size of each tapered microchannel gradually decreases along the channel from 100 to 10 µm, so that young adult worms are immobilized without the use of anesthesia, cooling or the use of glues. Several minutes after initiating the liquid flow, the worms filled up all the channels of the clamp and were immobilized. This process was not damaging to the worms, as previously reported (Hulme et al. 2007). As soon as the worms fill the channels of the clamp, the rest of the samples that were still in the inlet were aspirated with a vacuum pump and discarded. The inlet was then washed several times with M9 medium until no worms were visible under the microscope with the inlet in view. At this point, the worms in the channels were irradiated. After irradiation, the samples were released by reversing the flow direction in the syringe pump; within few minutes, irradiated worms migrated back to the loading reservoir and were collected for analysis with a manual pipettor and fresh M9 medium.

### Irradiation

For site-specific microbeam irradiation, individual worms were loaded into the worm clamp that was positioned using joystick control of the microbeam software. Each worm was then exposed to 4.5-MeV protons (LET ~9 keV/µm and range of 295 µm in water), with a beam diameter of 5 µm. Approximately 200 protons were delivered in the head-intestine area every 5 µm diagonally across the worm diameter using the Columbia University Radiological Research Accelerator Facility (RARAF) permanent magnet microbeam (Garty et al. 2006). In regard to beam scattering, the protons exit the vacuum via a 500-nm-thick $Si_3N_4$ window. They then traverse a thin air gap and enter the worm clamp via a 10-µm-thick PDMS film. The worms themselves are constrained by the height of the channel (40 µm). Prior to irradiation, the beam spot size was measured at the same plane as the bottom of the worm clamp, so only the additional scattering due to the PDMS and worm needs to be considered. SRIM calculations of 10 µm PDMS followed by 20 µm adipose tissue (ICRP ICRU-103) showed a beam broadening of about a quarter of a micron.

For broad-beam proton irradiation, 1 ml of young adult *C. elegans* in M9 was spread onto 35-mm Petri dishes and exposed to 0 or 10 Gy from 4.3-MeV protons (LET ~9 keV/µm) using the RARAF track segment facility (Geard et al. 2002). In every case, the exposures occurred at room temperature. The results are representative of three experiments; in the case of microbeam irradiations, an average of 50 samples was irradiated per experiment.

### Immunohistochemistry

One hour after irradiation, worms were analyzed for Rad51 foci formation by immunohistochemistry. Briefly, samples were prepared using the freeze–crack method (Duerr et al. 1999) using Superfrost Plus slides (Fischer Scientific, Pittsburg, PA) and then fixed for 5 min in −20 °C acetone (100 %) followed by 5 min in −20 °C methanol (100 %). Worms were then collected in 1× phosphate buffer saline (PBS) (Sigma, St. Louis, MO) and left overnight at 4 °C. Immunofluorescence staining was performed on fixed nematodes in suspension; samples were blocked for 30 min at room temperature in blocking solution (1 × PBS, 0.2 % fish gelatin, 0.25 % Triton) (Sigma, St. Louis, MO) and incubated overnight at 4 °C with primary anti-Rad51 antibody (14B4) (Novus Biological, Littleton, CO) (1:1,000 in blocking solution). Following five washes in washing solution (1× PBS, 0.25 % Triton) of 20 min each, worms were incubated for 3 h in secondary donkey anti-rabbit Alexa-555 antibody ($\lambda_{ex}/\lambda_{em}$ = 555/565 nm; Invitrogen, Grand Island, NY) (1:500 in blocking solution). Worms were washed as described above, mounted on clean glass slides in medium containing 5 mg/ml of 4′,6-diamidino-2-phenylindole (DAPI), and examined at a fluorescent microscope (Olympus IX70) equipped with filters and a Photometrics® PVCAM high-resolution, high-efficiency digital camera.

## Results and discussion

Although biological processes differ between mammals and *C. elegans*, regulatory and basic radiation-induced mechanisms seem to be conserved across species (Sakashita et al. 2010). For instance, *C. elegans* as well as mammals may respond to ionizing radiation by inducing p53-dependent apoptosis (Greiss et al. 2008). Similarly, radiation-induced bystander effects, which are well established in mammalian models (Morgan 2003a, b), have been recently described in nematodes (Sugimoto et al. 2006; Bertucci et al. 2009). Therefore, *C. elegans* is a very attractive model for in vivo investigations of tissue-specific effects induced by microbeam irradiation.

The use of a microbeam requires that samples remain immobile during irradiation; indeed, in previous microbeam protocols, worms were anesthetized (Bertucci et al. 2009). Other techniques to immobilize *C. elegans* as the use of glue (Kerr et al. 2000) are irreversible while others, including cooling (Stiernagle 1999), might interfere with the animal's normal physiological processes. Moreover, these methods to prevent worm movement during irradiation require that each sample has to be positioned by hand.

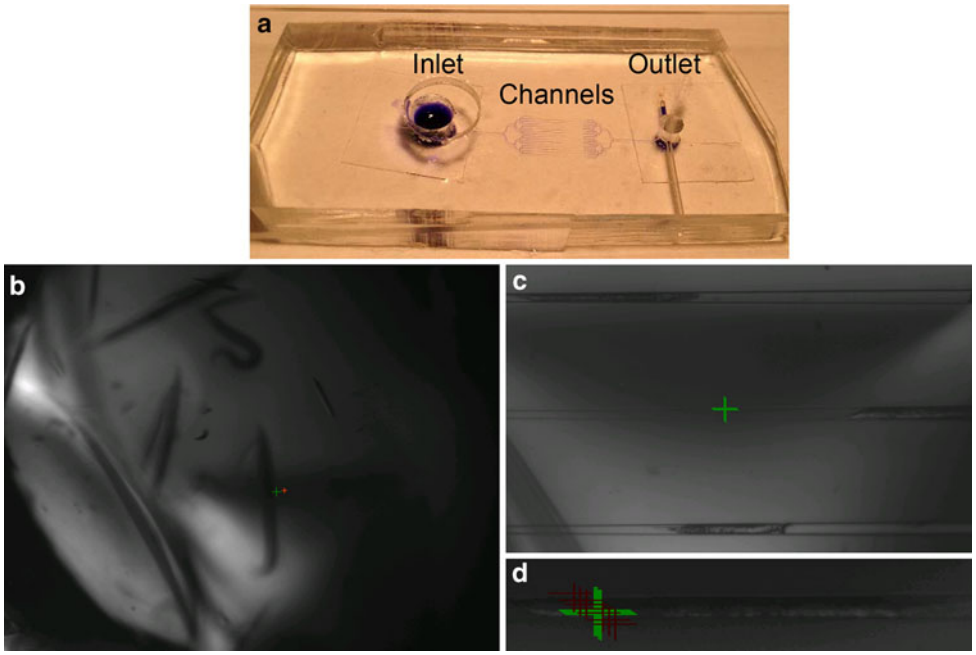


**Fig. 1** **a** A 16-channel microfluidic device for *C. elegans* observation and irradiation at the microbeam. **b** Once loaded in the inlet (10× view), worms move into the microfluidic channels through liquid flow between inlet and outlet. **c** The width of each microchannel gradually decreases along the 5-mm channel to 10 μm, so that young adult worms are immobilized without the use of anesthesia. Few minutes after initiating the liquid flow, the worms fill up the channels of the clamp (10× view). The *green cross* identifies the nominal location of the beam center and was used as a reference point for manual positioning of the worms. **d** Immobilized young adult worm at the time of irradiation (20× view). The *green cross* is the same as above. The *red crosses* show the actual targeted positions (color figure online)

To overcome these limitations and to support high-throughput irradiation of *C. elegans*, we have tailored a worm clamp (Hulme et al. 2007) to our microbeam irradiation setup (Garty et al. 2006). Microfluidic systems for observing *C. elegans* have been designed for imaging not immobilized worms (Lange et al. 2005, Kim et al. 2007) or worms that have been euthanized (Heng et al. 2006). In contrast, our microfluidic tool allows mechanical immobilization of multiple living *C. elegans*. We used these microfluidic devices to investigate in wild-type *C. elegans* the formation of Rad51 foci that promote repair of radiation-induced DSBs.

The target area for microbeam irradiation was chosen on the basis of whole-body irradiation experiments aimed at identifying the region of the worm exhibiting the most abundant formation of radiation-induced Rad51 foci (Martin et al. 2005). To this end, wild-type *C. elegans* were exposed to 0 or 10 Gy from $^{137}$Cs γ rays (data not shown). Compared to control, the area of the γ-irradiated worms that showed the highest amount of Rad51 foci corresponded to the head/intestine region (Martin et al. 2005), which was therefore chosen as the target site for exposure to the microbeam.

For microbeam irradiation, the samples were collected in centrifuge tubes by washing worm plates containing mostly young adult worms with 1–2 ml of sterile M9 buffer. Approximately 10-20 μl of the solution was dispensed in the inlet of the worm clamp (Fig. 1a) in order to load few dozen worms (Fig. 1b, 10× view). Since adult worms move at a very slow rate [∼200 μm per second (Karbowski et al. 2006)], they were gently transported into the microfluidic channels by liquid flow between inlet and outlet. Few minutes after initiating the liquid flow, the worms filled up the channels of the clamp; the width of each microchannel gradually decreases along the 5-mm channel down to 10 μm, so that young adult worms (50 μm in diameter) are mechanically immobilized. Subsequently, the worms were irradiated at the target of choice (Fig. 1c, d, 10× and 20× view, respectively. In both figures, the green cross identifies the nominal location of the beam center and was used as a reference point for manual positioning of the worms whereas the red crosses show the actual targeted positions.)

Once the worms were immobilized in the microfluidic clamp, the target area of each wild-type (N2) was exposed to 4.5-MeV protons as described above. As the wild-type *C. elegans* used in this study did not have a fluorescent marker in the target region, they were brought to the beam using a joystick under visual feedback. This could be automated, increasing targeting precision and irradiation throughput, if a fluorescent marker for the target of interest is available.

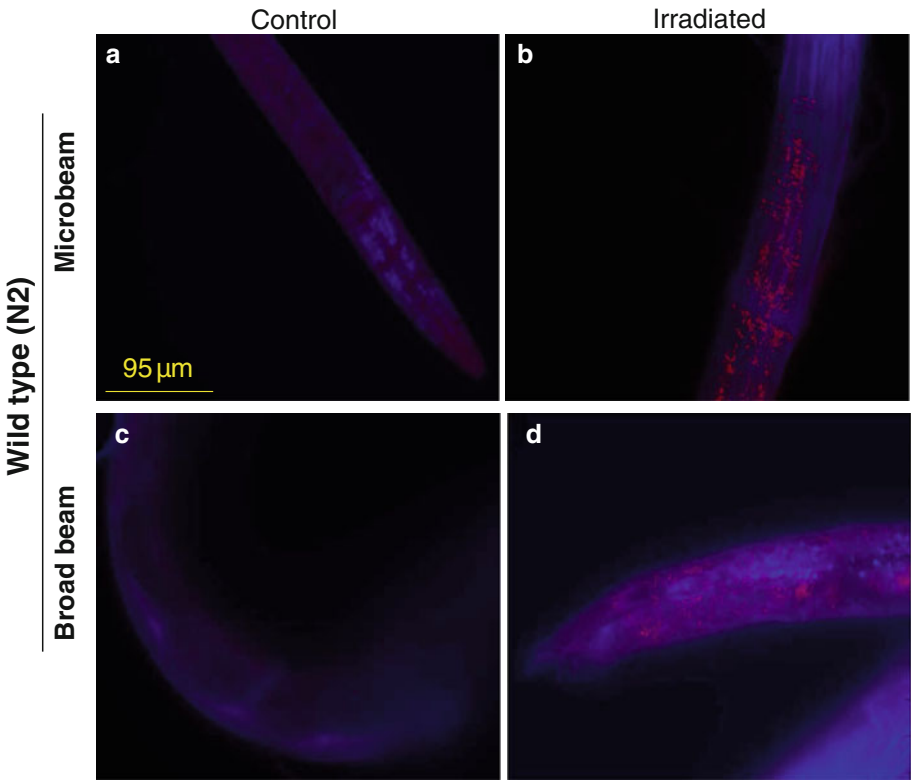


**Fig. 2** Rad51 foci formation in wild-type (N2) *C. elegans* exposed to **a** 0 or **b** 200 protons (4.5 MeV) delivered to the head/intestine area every 5 µm along the worm diameter (50 µm) or to **c** 0 or **d**10 Gy from broad-beam 4.3-MeV protons. Within 1 h after exposure, samples were analyzed for Rad51 foci formation by immunohistochemistry. Compared to respective control, microbeam irradiation of wild-type (N2) *C. elegans* in microfluidic channels showed an increase in Rad51 foci formation. *Blue* 4′,6-diamidino-2-phenylindole (DAPI); *Red* Alexa555-conjugated Rad51 secondary antibody. The *scale bar* pertains to all four panels (color figure online)

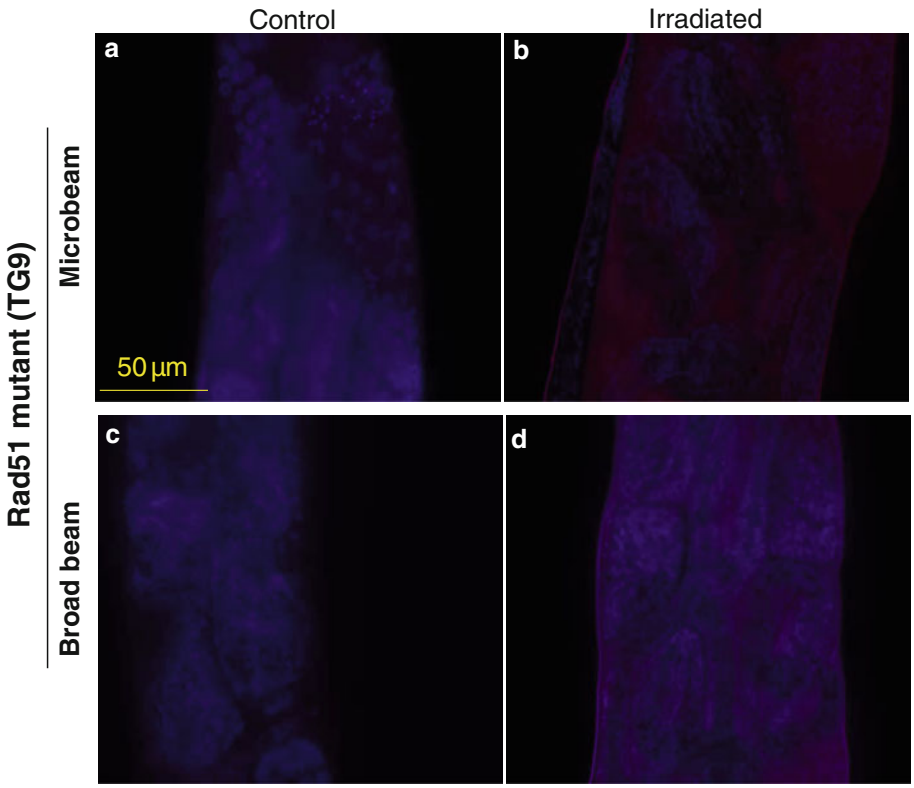


**Fig. 3** Rad51 foci formation in *rad51(Ig8701)* mutant *C. elegans* (strain TG9) exposed to **a** 0 or **b** 200 protons (4.5 MeV) delivered to the head/intestine area every 5 µm along the worm diameter (50 µm) or to **c** 0 or **d**10 Gy from broad-beam 4.3-MeV protons. Within 1 h after exposure, samples were analyzed for Rad51 foci formation by immunohistochemistry. Similar to respective controls, both microbeam- and broad-beam-irradiated mutants did not show unspecific binding to Rad51 protein forming foci. *Blue* = 4′,6-diamidino-2-phenylindole (DAPI); *Red* = Alexa555-conjugated Rad51 secondary antibody. The *scale bar* pertains to all four panels (color figure online)

After irradiation, the samples were released by reversing the flow direction in the syringe pump; within a few minutes, irradiated worms migrated back to the loading reservoir and were collected for analysis of Rad51 foci formation by immunohistochemistry that occurred 1 h after radiation exposure (Fig. 2). Compared to control (Fig. 2a), microbeam-irradiated wild-type (N2) worms showed an increase in Rad51 foci formation (Fig. 2b). To further confirm that foci formation was induced by proton irradiation, worms were exposed to 0 or 10 Gy from broad-beam protons (4.3 MeV, LET $\sim$9 keV/μm). Compared to respective control (Fig. 2c), broad-beam-irradiated N2 worms exhibited, mainly in the head/intestine region, an increase in Rad51 foci formation (Fig. 2d) that was similar to that observed in microbeam-irradiated samples (Fig. 2b).

To prove that Rad51 antibody had no unspecific binding, similar experiments were conducted in *rad51(Ig8701)* mutant worms (strain TG9) (Fig. 3). Compared to respective controls (Fig. 3a, c) and to microbeam-irradiated worms (Fig. 2b), both microbeam- and broad-beam-irradiated mutants did not show any unspecific binding to Rad51 protein forming foci (Fig. 3b, d, respectively).

Using a microfluidic device for microbeam irradiation of multiple living organisms at a time, our results indicate that 4.5-MeV protons induced DNA damage in wild-type *C. elegans*, as assessed by Rad51 foci formation.

Models such as *C. elegans* share cellular and molecular structures and control pathways with higher organisms; indeed, this system has been used to elucidate the underlying mechanisms of a number of human diseases (Levitan and Greenwald 1995; Lakso et al. 2003). *C. elegans* also allow expanding our basic knowledge of radiation-induced effects in whole living organisms (Sakashita et al. 2010). However, microbeam studies involving the irradiation of living organisms such as *C. elegans* are only beginning to emerge; site-specific irradiations of complex systems in which physiological conditions are preserved are critical in elucidating radiation-induced biological effects such as cell cycle arrest and apoptosis (Sugimoto et al. 2006) as well as bystander effects (Bertucci et al. 2009).

In conclusion, with an endpoint relevant to understanding the response of a whole organism to tissue-specific irradiation, here we showed that with our microfluidic device, we can perform precise and rapid microbeam irradiation of multiple *C. elegans* in parallel.

**Acknowledgments** This work was supported by the National Institute of Biomedical Imaging and Bioengineering (NIBIB) under Grant: 5 P41 EB002033 and an EMBO long-term fellowship and HFSPO long-term fellowship to M.G. We are grateful to the *Caenorhabditis* Genetics Center for providing the mutant strain. We thank the RARAF team for their scientific support and advice.

## References

Alpi A, Pasierbek P, Gartner A, Loidl J (2003) Genetic and cytological characterization of the recombination protein RAD-51 in *Caenorhabditis elegans*. Chromosoma 112(1):6–16

Bertucci A, Pocock RD, Randers-Pehrson G, Brenner DJ (2009) Microbeam irradiation of the *C. elegans* nematode. J Radiat Res 50(Suppl A):A49–A54

Brenner S (1974) The genetics of *Caenorhabditis elegans*. Genetics 77(1):71–94

Chung K, Crane MM, Lu H (2008) Automated on-chip rapid microscopy, phenotyping and sorting of *C. elegans*. Nat Methods 5(7):637–643

Duerr JS, Frisby DL, Gaskin J, Duke A, Asermely K, Huddleston D, Eiden LE, Rand JB (1999) The cat-1 gene of *Caenorhabditis elegans* encodes a vesicular monoamine transporter required for specific monoamine-dependent behaviors. J Neurosci 19(1):72–84

Durante M, Friedl AA (2011) New challenges in radiobiology research with microbeams. Radiat Environ Biophys 50(3): 335–338

Garty G, Ross GJ, Bigelow AW, Randers-Pehrson G, Brenner DJ (2006) Testing the stand-alone microbeam at Columbia University. Radiat Prot Dosimetry 122(1–4):292–296

Geard CR, Jenkins-Baker G, Marino SA, Ponnaiya B (2002) Novel approaches with track segment alpha particles and cell co-cultures in studies of bystander effects. Radiat Prot Dosimetry 99(1–4):233–236

Gilleland CL, Rohde CB, Zeng F, Yanik MF (2010) Microfluidic immobilization of physiologically active *Caenorhabditis elegans*. Nat Protoc 5(12):1888–1902

Goodhead DT (1994) Initial events in the cellular effects of ionizing radiations: clustered damage in DNA. Int J Radiat Biol 65(1):7–17

Greiss S, Schumacher B, Grandien K, Rothblatt J, Gartner A (2008) Transcriptional profiling in *C. elegans* suggests DNA damage dependent apoptosis as an ancient function of the p53 family. BMC Genomics 9:334

Greubel C, Hable V, Drexler GA, Hauptner A, Dietzel S, Strickfaden H, Baur I, Krucken R, Cremer T, Friedl AA, Dollinger G (2008) Quantitative analysis of DNA-damage response factors after sequential ion microirradiation. Radiat Environ Biophys 47(4):415–422

Heng X, Erickson D, Baugh LR, Yaqoob Z, Sternberg PW, Psaltis D, Yang C (2006) Optofluidic microscopy-a method for implementing a high resolution optical microscope on a chip. Lab Chip 6(10):1274–1276

Hulme SE, Shevkoplyas SS, Apfeld J, Fontana W, Whitesides GM (2007) A microfabricated array of clamps for immobilizing and imaging *C. elegans*. Lab Chip 7(11):1515–1523

Karbowski J, Cronin CJ, Seah A, Mendel JE, Cleary D, Sternberg PW (2006) Conservation rules, their breakdown, and optimality in *Caenorhabditis* sinusoidal locomotion. J Theor Biol 242(3): 652–669

Kerr R, Lev-Ram V, Baird G, Vincent P, Tsien RY, Schafer WR (2000) Optical imaging of calcium transients in neurons and pharyngeal muscle of *C. elegans*. Neuron 26(3):583–594

Kim N, Dempsey CM, Zoval JV, Sze J-Y, Madou MJ (2007) "Automated microfluidic compact disc (CD) cultivation system of *Caenorhabditis elegans*". Sens Actuators B Chem 122:511

Lakso M, Vartiainen S, Moilanen AM, Sirvio J, Thomas JH, Nass R, Blakely RD, Wong G (2003) Dopaminergic neuronal loss and motor deficits in *Caenorhabditis elegans* overexpressing human alpha-synuclein. J Neurochem 86(1):165–172

Lange D, Storment CW, Conley CA, Kovacs GTA (2005) A microfluidic shadow imaging system for the study of the nematode *Caenorhabditis elegans* in space. Sens Actuators B 107:904–914

Levitan D, Greenwald I (1995) Facilitation of lin-12-mediated signalling by sel-12, a *Caenorhabditis elegans* S182 Alzheimer's disease gene. Nature 377(6547):351–354

Lewis JA, Wu CH, Berg H, Levine JH (1980) The genetics of levamisole resistance in the nematode *Caenorhabditis elegans*. Genetics 95(4):905–928

Little JB (2000) Radiation carcinogenesis. Carcinogenesis 21(3): 397–404

Martin JS, Winkelmann N, Petalcorin MI, McIlwraith MJ, Boulton SJ (2005) RAD-51-dependent and -independent roles of a *Caenorhabditis elegans* BRCA2-related protein during DNA double-strand break repair. Mol Cell Biol 25(8):3127–3139

Morgan WF (2003a) Non-targeted and delayed effects of exposure to ionizing radiation: I. Radiation-induced genomic instability and bystander effects in vitro. Radiat Res 159(5):567–580

Morgan WF (2003b) Non-targeted and delayed effects of exposure to ionizing radiation: II. Radiation-induced genomic instability and bystander effects in vivo, clastogenic factors and transgenerational effects. Radiat Res 159(5):581–596

Mosconi M, Giesen U, Langner F, Mielke C, Dalla Rosa I, Dirks WG (2011) 53BP1 and MDC1 foci formation in HT-1080 cells for low- and high-LET microbeam irradiations. Radiat Environ Biophys 50(3):345–352

O'Rourke EJ, Conery AL, Moy TI (2009) Whole-animal high-throughput screens: the *C. elegans* model. Methods Mol Biol 486:57–75

Rinaldo C, Bazzicalupo P, Ederle S, Hilliard M, La Volpe A (2002) Roles for *Caenorhabditis elegans* rad-51 in meiosis and in resistance to ionizing radiation during development. Genetics 160(2):471–479

Rohde CB, Zeng F, Gonzalez-Rubio R, Angel M, Yanik MF (2007) Microfluidic system for on-chip high-throughput whole-animal sorting and screening at subcellular resolution. Proc Natl Acad Sci USA 104(35):13891–13895

Rothman JH, Singson A (2012) *Caenorhabditis elegans*. Cell Biol Physiol

Sakashita T, Takanami T, Yanase S, Hamada N, Suzuki M, Kimura T, Kobayashi Y, Ishii N, Higashitani A (2010) Radiation biology of *Caenorhabditis elegans*: germ cell response, aging and behavior. J Radiat Res 51(2):107–121

Shi W, Wen H, Lin B, Qin J (2011) Microfluidic platform for the study of *Caenorhabditis elegans*. Top Curr Chem 304:323–338

Shinohara A, Ogawa T (1995) Homologous recombination and the roles of double-strand breaks. Trends Biochem Sci 20(10): 387–391

Stiernagle T (1999) *C. elegans* maintenance. *C. elegans*: a practical approach. I. A. Hope. Oxford University Press, Oxford

Sugimoto T, Dazai K, Sakashita T, Funayama T, Wada S, Hamada N, Kakizaki T, Kobayashi Y, Higashitani A (2006) Cell cycle arrest and apoptosis in *Caenorhabditis elegans* germline cells following heavy-ion microbeam irradiation. Int J Radiat Biol 82(1):31–38

Sung P (1994) Catalysis of ATP-dependent homologous DNA pairing and strand exchange by yeast RAD51 protein. Science 265(5176):1241–1243

Takanami T, Sato S, Ishihara T, Katsura I, Takahashi H, Higashitani A (1998) Characterization of a *Caenorhabditis elegans* recA-like gene Ce-rdh-1 involved in meiotic recombination. DNA Res 5(6):373–377

Takanami T, Mori A, Takahashi H, Higashitani A (2000) Hyper-resistance of meiotic cells to radiation due to a strong expression of a single recA-like gene in *Caenorhabditis elegans*. Nucleic Acids Res 28(21):4232–4236

Ward JF (1995) Radiation mutagenesis: the initial DNA lesions responsible. Radiat Res 142(3):362–368

Xia Y, Whitesides GM (1998) Soft lithography. Angew Chem Int Ed Vol 37(5):550–575

Zeng F, Rohde CB, Yanik MF (2008) Sub-cellular precision on-chip small-animal immobilization, multi-photon imaging and femtosecond-laser manipulation. Lab Chip 8(5):653–656